Final Report: Investigating Photovoltaic Solar Cells for Efficiency Improvements

Kara Ferner

April 28, 2021

Dr. Peter Monaghan

Faculty Advisor

Abstract

As the global demand for electricity has continued to increase, it is vital that we find clean, renewable energy sources to replace our reliance on nonrenewable energy. One potential solution is photovoltaics, which is the use of semiconductors to generate electricity from the sun and is more commonly referred to as solar panels. But in order for photovoltaics to compete with traditional sources of energy, its efficiency must be improved. Currently, research is being conducted to better optimize the performance of photovoltaics under different conditions. This project aims to investigate how different photovoltaics respond to varying conditions of solar irradiance and temperature. By comparing experimental data of two types of small silicon solar panels to simulation data using LabVIEW software, this project serves to identify limitations to current photovoltaics. The data analysis led to suggest that solar irradiance has a positive correlation to output power. Additionally, analyzing the effect of temperature on panel efficiency led to suggest that while temperature can have a positive correlation to efficiency for panels with lower current and higher voltage, further data analysis showed that higher temperatures may actually have negative effects on panels with higher current and lower voltage (i.e. panels typically of larger sizes used for homes, industry, etc.). Practical implications and areas for future research were suggested based on the results of this project.

Introduction

With a growing population and limited amount of nonrenewable energy sources available, finding alternative options for energy will be crucial for sustainable consumption. One of the most promising solutions is **photovoltaic** (PV) solar power. PV solar cells are made of semiconducting material in a p-n junction that utilizes the photoelectric effect to produce electricity from the sunlight [1]. Making up most of the typical solar panels available today, PV solar power is advantageous for many reasons: it is clean, silent, and easy to maintain. But when compared to traditional sources of energy such as natural gas, coal, or nuclear

power, PV solar power suffers significant drawbacks in efficiency. For a solar cell, efficiency is the ratio of the output power generated by the cell to the total input power from the sun. More efficient PV cells can better convert the sun's energy into electricity, while less efficient PV cells lose a significant portion of incoming power resulting in a production of less electricity.

In 1961, two scientists William Shockley and Hans J. Queisser formulated the Shockley-Quiesser limit, which stated that the maximum theoretical efficiency for a single p-n junction solar cell (i.e. a typical photovoltaic system) is about 30% and occurs at an optimal band gap for the semiconducting material of about 1.1 eV [2]. More recently, in 2016, a maximum efficiency for a single p-n junction was found to increase to 33.7% with a bandgap of 1.34 eV [3]. When PV cells were first produced, the recorded efficiencies were less than 5%, but over time efficiencies have increased and costs have become cheaper. Today, the highest efficiencies recorded are around 26-29%, achieved by cells made from various types of silicon or cells made from gallium arsenide [4]. However, because there is still room for improvement to reach the theoretical limit, physicists, engineers, chemists, and materials scientists alike are continuing large research efforts to maximize efficiency of solar cells.

The goal of this project is to identify optimal conditions for and assess potential limits to practical solar cell efficiency. The project aims to answer those questions by comparing experimental data of two small photovoltaic (PV) solar panels to simulation data collected using LabVIEW (Laboratory Virtual Instrument Engineering Workbench). The design of this project is best described in two data-taking portions: the experimental component provides "actual" values and the simulation component provides "theoretical" values. The data analysis of this project connects the two key portions, providing direct comparison through percent errors and graphs.

The experimental portion of this project consisted of testing a monocrystalline silicon (m-Si) and a polycrystalline silicon (p-Si) solar panel. Several sets of panel output data were collected for each panel at different conditions of both solar irradiance and temperature. The

simulation data was collected using a LabVIEW program created to produce the theoretical output of a PV cell. The simulation was purely based on the mathematical model derived from the equivalent circuit representation of a PV cell. The data analysis provided a numerical and graphical comparison of the experimental data to the simulation data for values of: maximum output power, voltage at maximum power, current at maximum power, optimal load resistance, and efficiency percentage, η.

The expected results hypothesized at the start of this project were:

1. Actual $\eta <$ theoretical η
2. p-Si $\eta <$ m-Si η
3. η decreases as solar irradiance decreases
4. η decreases as temperature increases

Theory

PV solar panels are comprised of individual cells, and each individual PV cell is made of semiconducting material. Semiconductors are used for PV cells because they allow for the photoelectric effect, the process by which photons from incoming sunlight interact with the electrons in the material to produce electricity. When photons hit the semiconducting material, their energy causes excitation of electrons. A photon has an energy of $E = hf$, where h is Planck's constant and f is the wave frequency of the photon. Each semiconducting material has a characteristic band gap, often given in units of electron-volts (eV), that describes how much energy is required to excite an electron from the valence band up to the conduction band [1, 5]. If the photon energy is equal to the band gap of the material, the photon's interaction with an electron will cause it to be sent to the conduction band where it becomes a free electron.

The specific design of semiconducting material in PV cells makes use of these free electrons. Each PV cell is typically formed as a single p-n junction, like a diode. In the case of silicon, its four valence electrons result in a nice lattice structure, but by "doping" silicon with other elements, a junction can be produced that is conducive for generating an electric field. In the context of semiconductors, "doping" refers to the process of injecting other elements or compounds into the material to cause intentional modifications of properties [1, 5]. The n-type region, for example, can be made by injecting phosphorous into the silicon. Since phosphorus has five valence electrons, the resulting formation will have extra electrons. On the other hand, the p-type region can be produced by an injection of something like boron, with only three valence electrons. Here, the absence of electrons results in "holes" that can effectively be thought of as positive charges. When placed next to each other, the free electrons from the n-type region will fill the holes in the p-type region. This results in what is known as the depletion zone: positively charged ions in the n-type region and negatively charged ions in the p-type region, producing an electric field as shown in Figure 1. Then when placed under a light source, photons carrying enough energy will free up electrons that can then move according to the electric field, generating a current [1, 5].

Two parameters that are very significant in the analysis of solar cells are open-circuit voltage, V_{oc}, and short-circuit current, I_{sc}. V_{oc} is the maximum voltage that can be read from a solar cell, found when $I = 0$, while I_{sc} is the maximum current that can be read from a solar cell found when $V = 0$; however, a PV solar cell can never actually operate (i.e., generate any electricity) at either open-circuit voltage or short-circuit current because the power ($P = IV$) at both of these points is then also zero [7]. Thus, a PV solar cell's point of maximum power actually occurs at some slightly smaller voltage and current, V_{mp} and I_{mp}, respectively, where $P_{max} = V_{mp}I_{mp}$. Then efficiency of a solar panel is given by the ratio of power-out to power-in:

$$\eta = \frac{P_{max}}{P_{in}} = \frac{V_{mp}I_{mp}}{P_{in}} \tag{1}$$

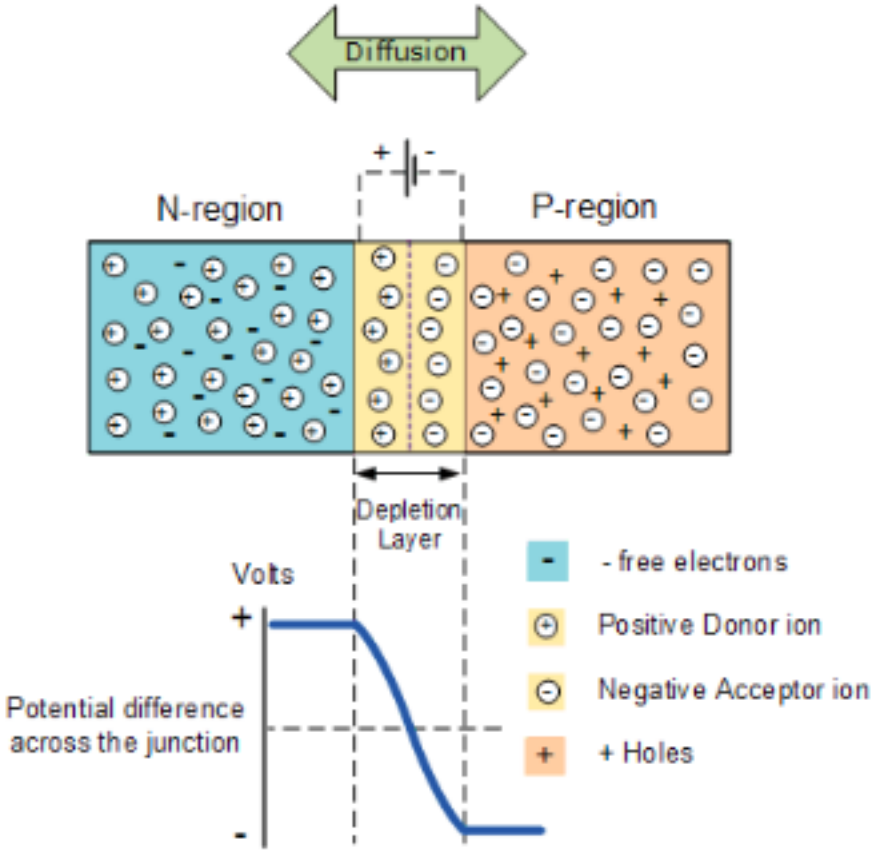

Figure 1: p-n junction of a semiconducting material [6]

Then, by calculating P_{in} as the area of the solar cell (m^2) multiplied by the solar irradiance (W/m^2), the efficiency η can be found for a given data measurement of a solar panel [8, 9].

The voltage, current, and power characteristics of PV solar cells are also often presented in a graphical format, specifically as a current vs. voltage (I-V) plot and a power vs. voltage (P-V) plot, shown in Figure 2. Every PV solar cell should have I-V and P-V curves of this characteristic shape. Examining these plots clearly shows where a maximum power point can be located, and that this point is always at some voltage and current slightly less than V_{oc} and I_{sc}. Also, rearranging Ohm's Law to $I = \frac{V}{R}$ and recognizing that current and voltage can be related by a line of slope $\frac{1}{R}$, we see different values of load resistance R create lines of different slopes that intersect the I-V curve at different points, shown in Figure 3. This shows that one way of finding the maximum power point at $V = V_{mp}$ and $I = I_{mp}$ is to find the value of load resistance that optimizes output power. This value of load resistance will be referred to as the optimal load resistance, $R = R_{opt}$.

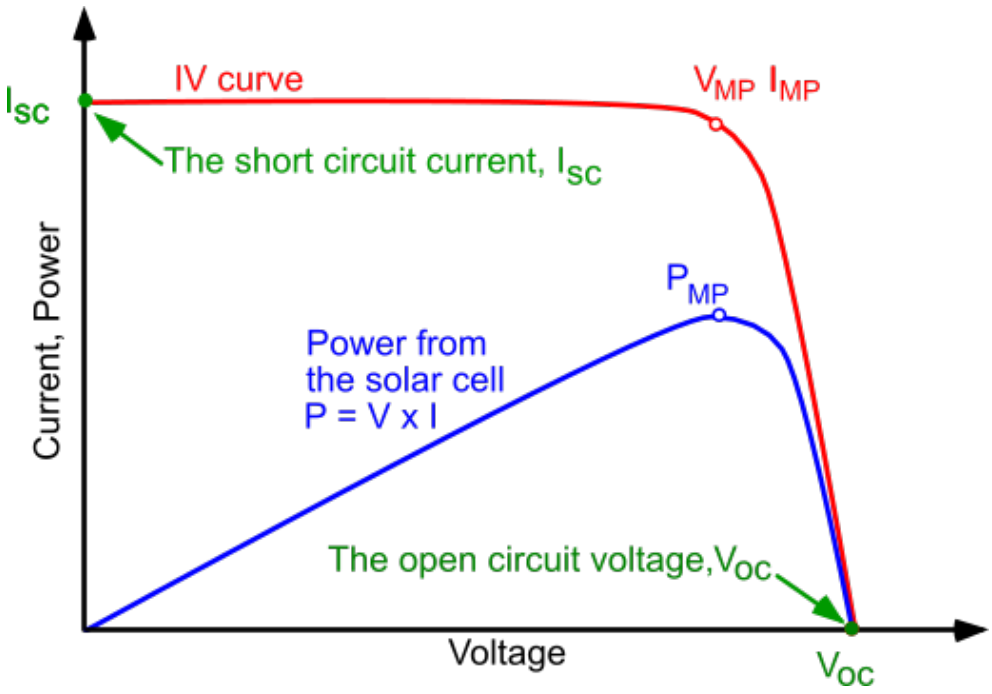

Figure 2: I-V and P-V curves of a solar panel [10]

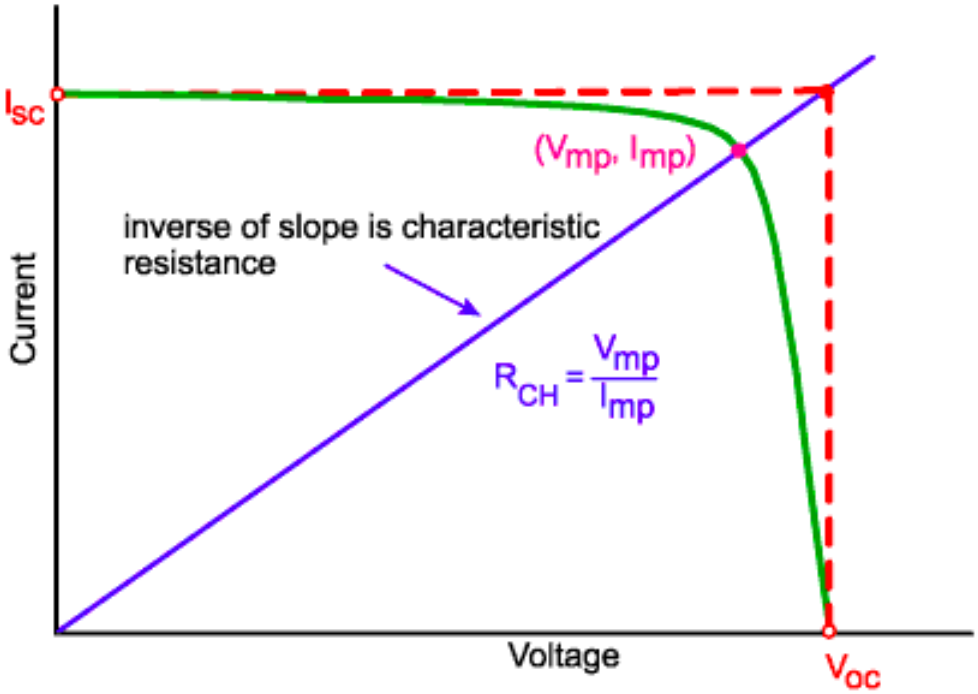

Figure 3: I-V curve of a solar panel showing optimal load resistance relationship [11]

Methods

Experimental

The experimental portion of this project involved collecting several sets of data for two types of small PV solar panels: a polycrystalline silicon panel and a monocrystalline silicon panel. For each data set, the solar irradiance was measured using a digital handheld pyranometer and the temperature was measured using the temperature setting of a multimeter. Each data set was then definied by panel type, solar irradiance, and temperature.

The process for collecting each set of data was to measure the output of the panel across different values of load resistance, with the purpose of finding the maximum output power and identifying that associated value of optimal load resistance. The steps are as follows:

1. After measuring and recording the conditions, the first step for each set of data was to measure the open-circuit voltage and short-circuit current. The open-circuit voltage and short-circuit current were then used with Ohm's Law ($V = IR$) to calculate an estimate for the optimal load resistance.

2. With the multimeter on the ohmmeter setting, the resistance of the potentiometer was set to a specific resistance, and this value was recorded.

3. The potentiometer and multimeter were connected in parallel to the panel, and output voltage was measured and recorded.

4. The potentiometer and multimeter were connected in series to the panel, and output current was measured and recorded.

5. Output power was calculated by multiplying output voltage and current, $P = VI$.

6. Steps 2-5 were repeated for each change of the potentiometer resistance, adjusting the potentiometer up or down slightly based on the previous output power. Once

the change in output power was limited by the potentiometer's sensitivity, the final value for the maximum power point and it's associated optimal load resistance, output voltage, and output current were identified. Data points were collected for a range of resistance values from nearly 0 Ω to nearly 100 Ω.

Simulation

The simulation portion of this project consisted of creating a program in LabVIEW. LabVIEW was chosen as the preferred programming language for this project primarily due to its graphical interface as a "G" programming language. The LabVIEW program runs as a virtual instrument (VI) which contains two components: a block diagram and a front panel. The block diagram portrays the entire source code of the program (from input to output) in a graphical format while the front panel displays all of the input and output components as a user interface. The block diagram of the LabVIEW program can be found in the Appendix at the end of this report. For this project, input values will be entered to simulate each of the experimental data sets, generating a set of "theoretical" values for each set of "actual" values and providing supplementary I-V and P-V plots to help visualize the data.

The LabVIEW simulation is based on the mathematical model derived from the equivalent circuit representation of a PV cell. As shown in Figure 4, a PV cell of a single p-n junction can be represented as a current source in parallel with a diode element [8]. There are two parasitic resistances to be considered. R_s represents the series resistance, which inevitably occurs due to contact between metal and the semiconducting silicon. A larger value for series resistance results in power losses because it lowers the amount of output current traveling to the terminal. R_{sh} represents the shunt resistance, which can occur due to manufacturing defects. When the shunt resistance is a low value, as can be observed by the circuit diagram, it causes a "leakage" of current by providing an alternate path for the current to travel. Thus, low shunt resistance also results in significant power losses. In an ideal PV cell, there would be no series resistance ($R_s = 0$) and the shunt resistance would

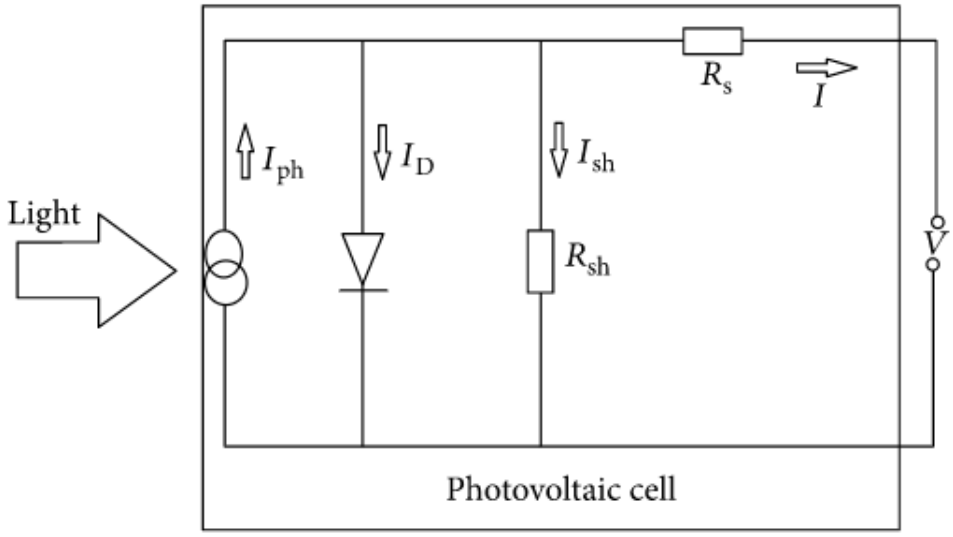

Figure 4: Equivalent Circuit Representation of a PV Solar Cell [12]

approach infinity ($R_{sh} = \infty$) [7, 8].

As shown in Figure 4, I is the output current at the terminal and can be found using Kirchoff's current law:

$$I = I_{ph} - I_D - I_{sh} \tag{2}$$

where I_{ph} is the photogenerated current, or the current that is generated from the initial interaction between the photons and electrons, I_D is the diode current, and I_{sh} is the current through the shunt resistance [8].

The current across the diode can be replaced by the Shockley Ideal Diode Equation,

$$I_D = I_o \left(e^{\frac{qV_D}{nkT_c}} - 1 \right) \tag{3}$$

where q is the charge of an electron, k is the Boltzmann constant, n is the "ideality factor" of the cell (a value between 1 and 2, determined by the manufacturer), T_c is the temperature of the cell, and V_D is the voltage across the diode [9, 13]. I_o is the dark-saturation current of the diode, which represents the leakage of current that occurs in the absence of light and depends on the band gap of the material [8]. Also, using the laws of circuits, the current

across the shunt resistance is:

$$I_{sh} = \frac{V + IR_s}{R_{sh}} \tag{4}$$

and the voltage across the diode element is:

$$V_D = IR_s + V \tag{5}$$

Lastly, because there is no terminal voltage in a short circuit ($V = 0$), the short-circuit current is equal to the photogenerated current:

$$I_{sc} = I_{ph} \tag{6}$$

Replacing these equations into Equation 2 for output current gives the important "PV Equation" that relates output current to output voltage:

$$\boxed{I = I_{sc} - I_o \left(e^{\frac{q(V+IR_s)}{nkT_c}} - 1 \right) - \frac{V + IR_s}{R_{sh}}} \tag{7}$$

In LabVIEW, there are a few steps of calculation required first before being able to fully examine the "PV Equation." The input values needed for the simulation are: the temperature of the cell (T_c) in Kelvin, a chosen reference temperature (T_r) in Kelvin, short-circuit current at the reference temperature (I_{scr}) in Amps, open-circuit voltage at the reference temperature (V_{ocr}) in Volts, the solar irradiance (G) in Watts per meter squared, series resistance (R_s) in Ohms, shunt resistance (R_{sh}) in Ohms, an estimate for load resistance (R_{load}) in Ohms, the band gap of the material (E_g) in electron-volts, the "ideality factor" of the cell (n), and the temperature coefficient (K_i) that characterizes the power loss for a given material per increase in degrees Celcius [9]. Relevant constants that will also serve as input values are the charge of an electron ($q = 1.6 \times 10^{-19}$ C) and the Boltzmann constant ($k = 1.38 \times 10^{-23}$ J/K).

Since the manufacturer provided short-circuit current and open-circuit voltage for each

panel at standard test conditions (solar irradiance of 1000 W/m^2 and temperature of 298.15 K), this project used 298.15 K for reference temperature T_r and used the manufacturers data for I_{scr} and V_{ocr}. Because a PV cell would ideally have a shunt resistance approaching infinity and a series resistance approaching zero, shunt resistance was set to 5000 Ω and the series resistance was set to 5×10^{-5} Ω for this simulation. Polycrystalline silicon loses about 0.4%-0.5% of efficiency for every increase °C, so a generally accepted value for the temperature coefficient, K_i, for polycrystalline silicon is 0.005. Meanwhile, since monocrystalline silicon is of slightly better quality, it has a temperature coefficient of about 0.0035 [12]. Additionally, silicon has a band gap of $E_g = 1.12$ eV and a generally accepted value for the "ideality factor" of silicon solar panels is $n = 1.3$ [4, 12].

Using these input values, the preliminary calculations are are given in Steps 1-3:

1. Short-circuit current is calculated depending on the solar irradiance and temperature, given by:

$$I_{sc} = \frac{G}{1000} \left[I_{scr} + K_i \left(T_c - T_r \right) \right] \tag{8}$$

2. Next, the reverse-saturation current of the diode, I_{or}, is found by Equation 9, then used to find the dark-saturation current, I_o, given by Equation 10 [8, 9].

$$I_{or} = \frac{I_{scr}}{e^{\frac{qV_{ocr}}{nkT_r}} - 1} \tag{9}$$

$$I_o = I_{or} \left(\frac{T_c}{T_r} \right)^{3/n} exp \left(\frac{qE_g}{nk} \left(\frac{1}{T_c} - \frac{1}{T_r} \right) \right) \tag{10}$$

3. Finally, open-circuit voltage, V_{oc}, can be derived from setting $I = 0$ in the "PV Eqaution" (Equation 7) [8, 9].

$$V_{oc} = \left(\frac{nkT_c}{q} \right) ln \left[\frac{I_{sc}}{I_o} + 1 \right] \tag{11}$$

After calculating $I_{sc}, I_{or}, I_o,$ and V_{oc}, the "PV Equation" given by Equation 7 is analyzed; however, because it is a transcendental equation, there is no closed-form solution for output current, I.

4. In LabVIEW, a for-loop structure was used for modeling the the "PV equation." The for-loop essentially produces an integration for current by plugging in incremental values of voltage for each iteration of the for-loop. Depending on the desired precision of the method, the number of iterations of the for-loop can be altered. It requires an estimated or expected value to be input for the optimal load resistance, R_{load}, so that the variable for current I on the right-hand-side of Equation 7 can be replaced with V/R_{load}.

5. For each iteration of the for-loop, the values generated for voltage, current, and power were added to their specific arrays. The built-in LabVIEW array functions were then used to find the maximum value in the power array and its associated index.

6. The identified index of maximum power was then used as an input for the voltage and current arrays to access the voltage at maximum power, V_{mp}, and the current at maximum power, I_{mp}.

7. Then the optimal value for load resistance, R_{opt}, was calculated using Equation 12 and the efficiency percentage, η was calculated using Equation 13.

$$R_{opt} = \frac{V_{mp}}{I_{mp}} \tag{12}$$

$$\eta = \frac{P_{out}}{P_{in}} = \frac{V_{mp} I_{mp}}{\text{cell surface area} \times \text{solar irradiance}} \tag{13}$$

8. The last step of the LabVIEW simulation was to use the arrays of current and voltage to create an I-V plot and to use the arrays of power and voltage to create a P-V plot.

Data Analysis

The data analysis for this project took several forms. The first was to compare experimental values to the simulation values. Relevant values for this comparison were maximum output power, voltage at maximum power, current at maximum power, optimal load resistance, and efficiency. For each set of data, percent errors were calculated for each of these five values, assuming the experimental values were the "actual" values and the simulation values were the "theoretical" values. The formula for percent error is given in Equation 14.

$$\text{Percent Error} = \frac{\text{theoretical value} - \text{actual value}}{\text{theoretical value}} \times 100 \tag{14}$$

However, the most interesting data analysis came from the graphical portion. Again, to compare experimental values to simulation values, graphs were plotted to explore trends in some of the output values based on solar irradiance or temperature. Finally, data analysis was also used to isolate either the experimental portion or the simulation portion, to examine more specifically how solar irradiance or temperature affect the I-V or P-V curves.

Data

All experimental data was recorded using Google Sheets. After gathering a few data sets for each panel, the I-V and P-V characteristic plots were generated within Google Sheets. For both the polycrystalline and monocrystalline panel, the shapes of the curves follow the expected I-V and P-V trends. For each panel, plots of the I-V and P-V curves for a single set of data can be seen in Figures 5, 6, 7, 8.

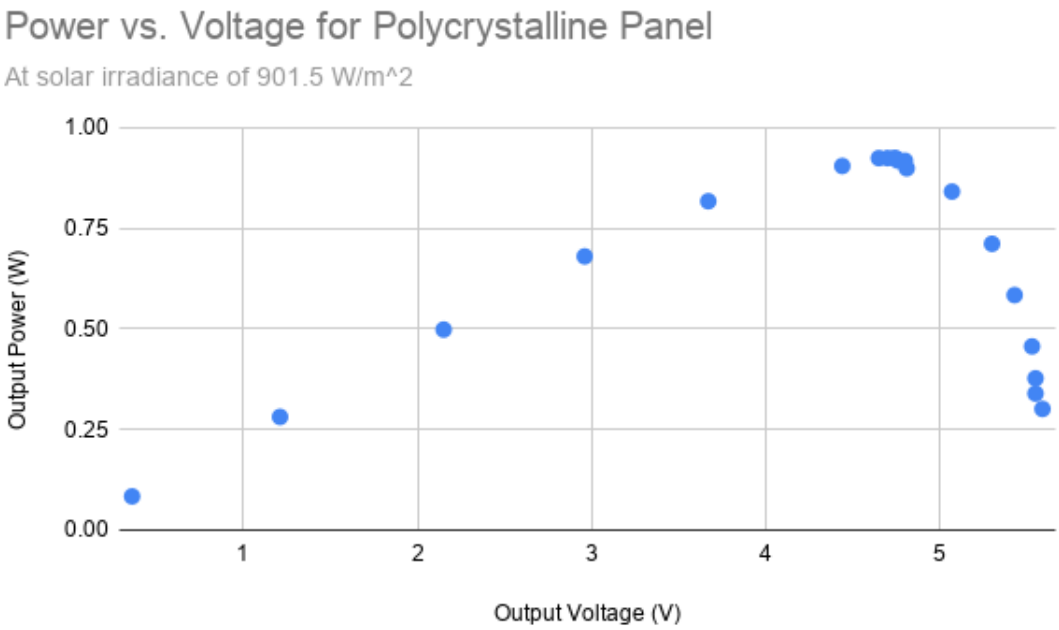

Figure 5: P-V Plot for Polycrystalline Panel

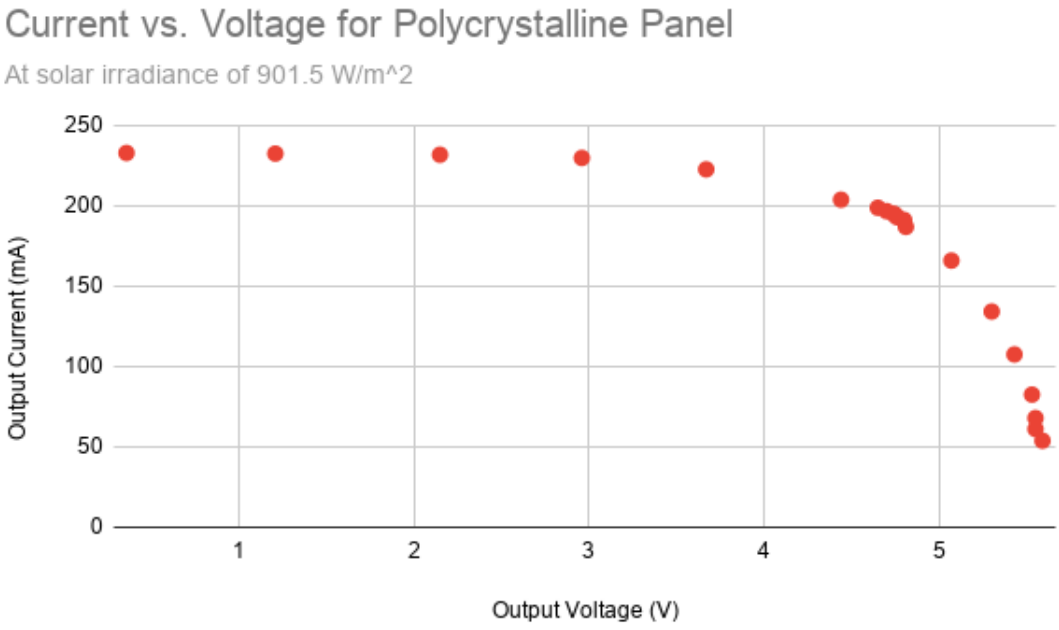

Figure 6: I-V Plot for Polycrystalline Panel

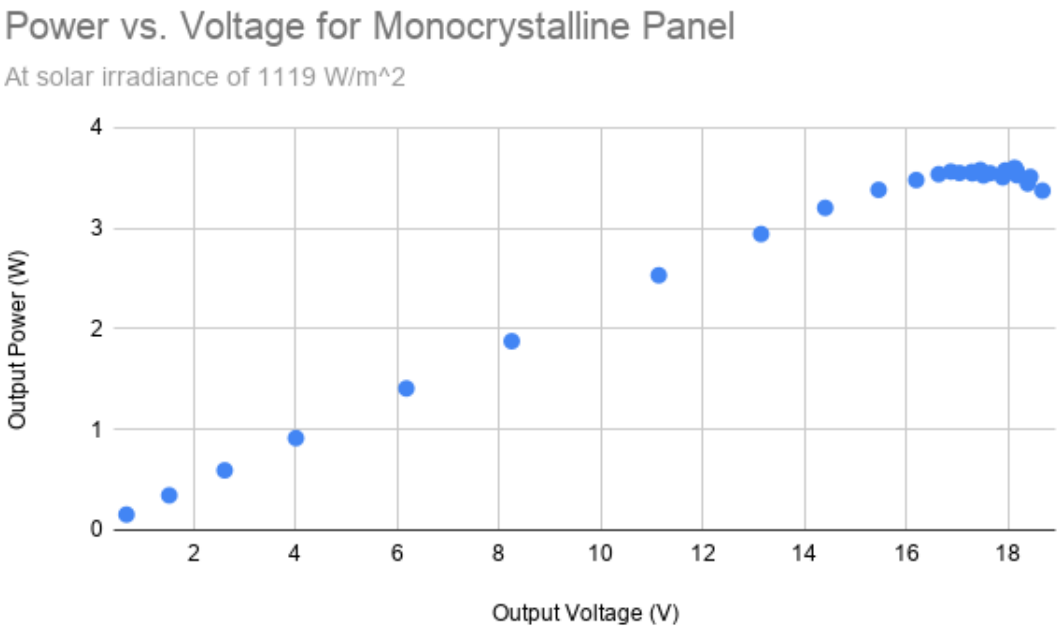

Figure 7: P-V Plot for Monocrystalline Panel

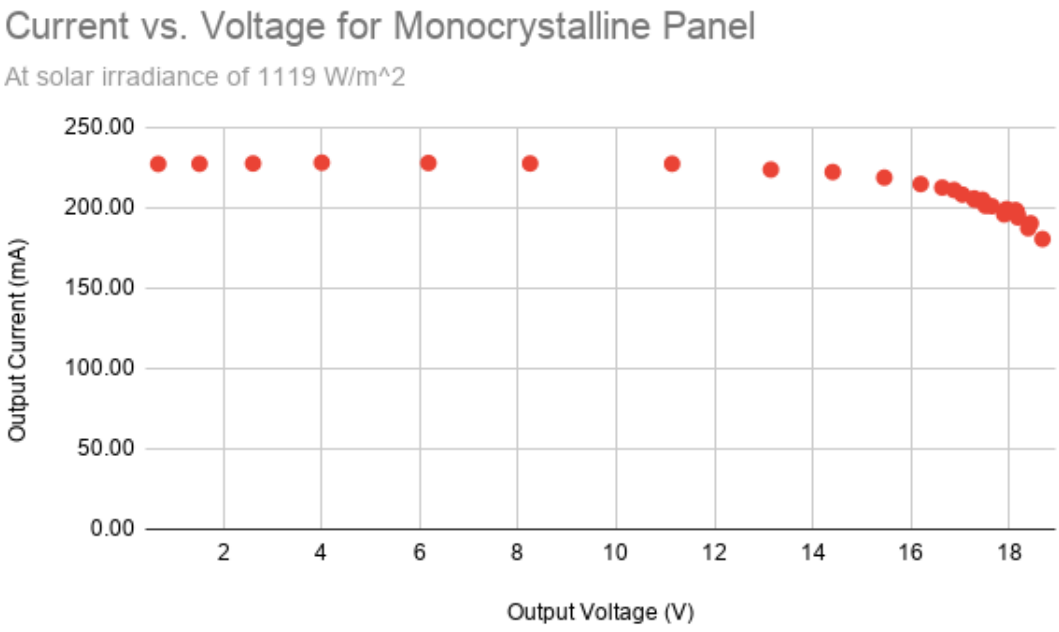

Figure 8: I-V Plot for Monocrystalline Panel

In Figures 5 and 6 for the polycrystalline panel, it is shown that there exists some maximum power point that occurs at a voltage slightly less than open-circuit voltage and a current slightly less than short-circuit current. The short-circuit current is represented where the I-V curve intersects the y-axis (i.e. where V=0) and the open-circuit voltage is represented where the I-V curve intersects the x-axis (i.e. where I=0). Similarly, a maximum power point can also be seen in the plots for the monocrystalline panel shown in Figures 7 and 8. However, the location of the open-circuit voltage is not as obvious in these plots since more data points were not obtainable at higher voltages. This is because the potentiometer used in experiment had a maximum value of 100 Ω, which was sufficient to finding the maximmum power for both panels, but given that the monocrystalline panel had a much higher open-circuit voltage, its optimal load resistance was much higher than that of the polycyrstalline panel. For these particular data sets, the polycrystalline panel produced a maximum power output of 0.925248 W, at a voltage of 4.74 V and a current of 195.2 mA with the optimal load resistance of 21.6 Ω; the monocrystalline panel produced a maximum power output of 3.602431 W, at a voltage of 18.13 V and a current of 198.7 mA with the optimal load resistance of 88.6 Ω.

More data sets were obtained for both panels at varying values of solar irradiance. The polycyrstalline P-V and I-V curves for five data sets of different values of solar irradiance were plotted on the same graph, showing how the current and power characteristics change with solar irradiance. Figure 9, shows how the maximum output power decreases as solar irradiance decreases, while a change in solar irradiance has little effect on the value of open-circuit voltage. Figure 10 shows how short-circuit current also decreases as solar irradiance decreases.

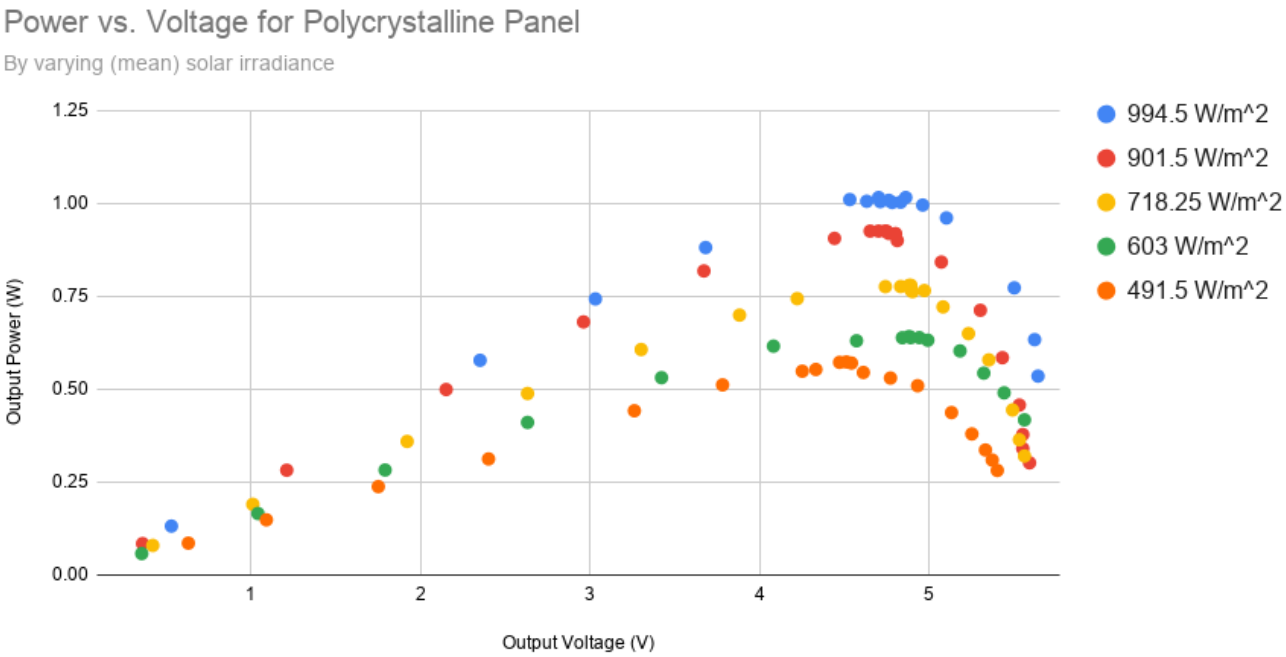

Figure 9: P-V Plots of Multiple Data Sets for Polycrystalline Panel

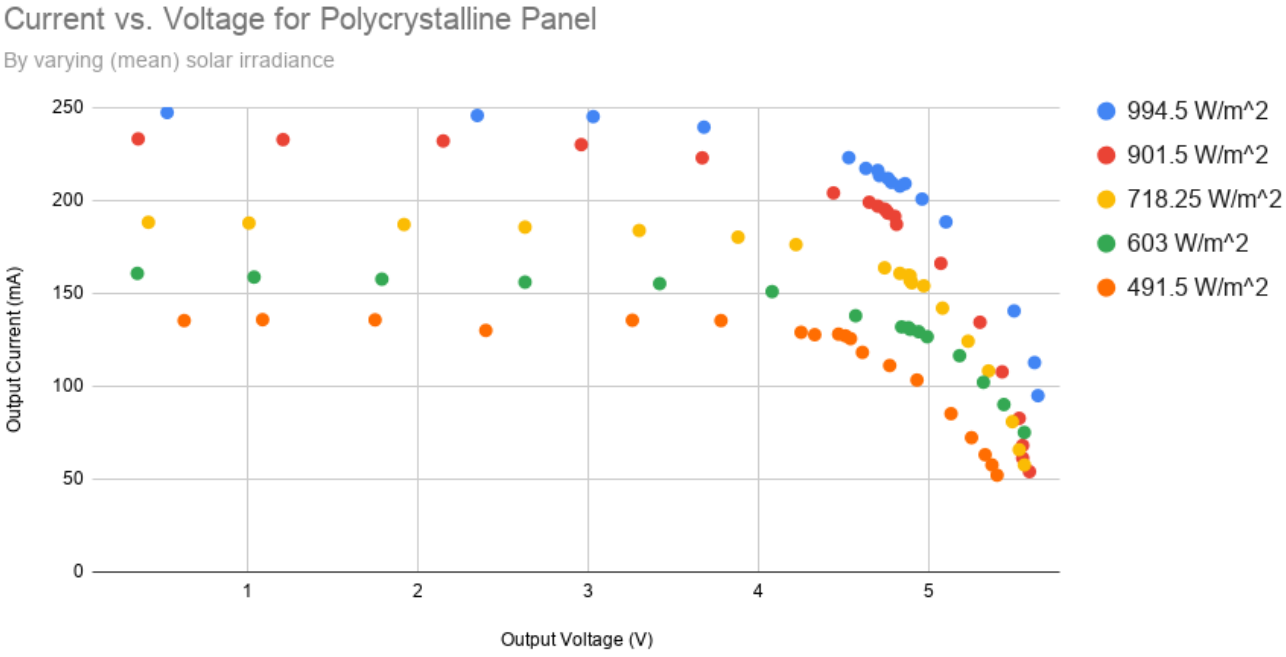

Figure 10: I-V Plots of Multiple Data Sets for Polycrystalline Panel

Similarly, the P-V and I-V curves for three different data sets of varying solar irradiance for the monocrystalline panel are shown in Figures 11 and 12. The monocrystalline panel also shows a decrease in maximum output power and short-circuit current with a decrease in solar irradiance. The change between plots is less drastic due to smaller changes in solar irradiance. Other data sets at lower values of solar irradiance were not possible for the monocrystalline panel due to needing a larger load resistance value than the potentiometer's 100 Ω limit. This is because with such a high open-circuit voltage, at lower solar irradiance values that generate less current, the value of optimal load resistance to find maximum output power, $R = \frac{V}{I}$, becomes very large. Nonetheless, the direct relationship between maximum power output and solar irradiance is still apparent.

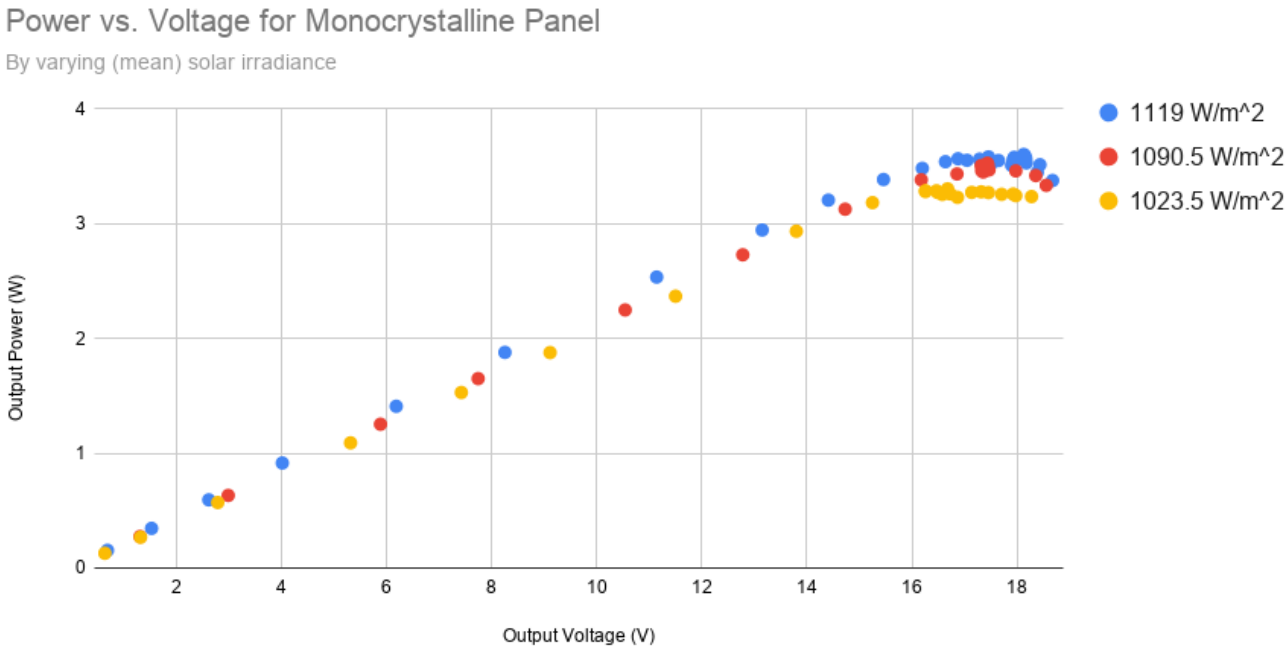

Figure 11: P-V Plots of Multiple Data Sets for Monocrystalline Panel

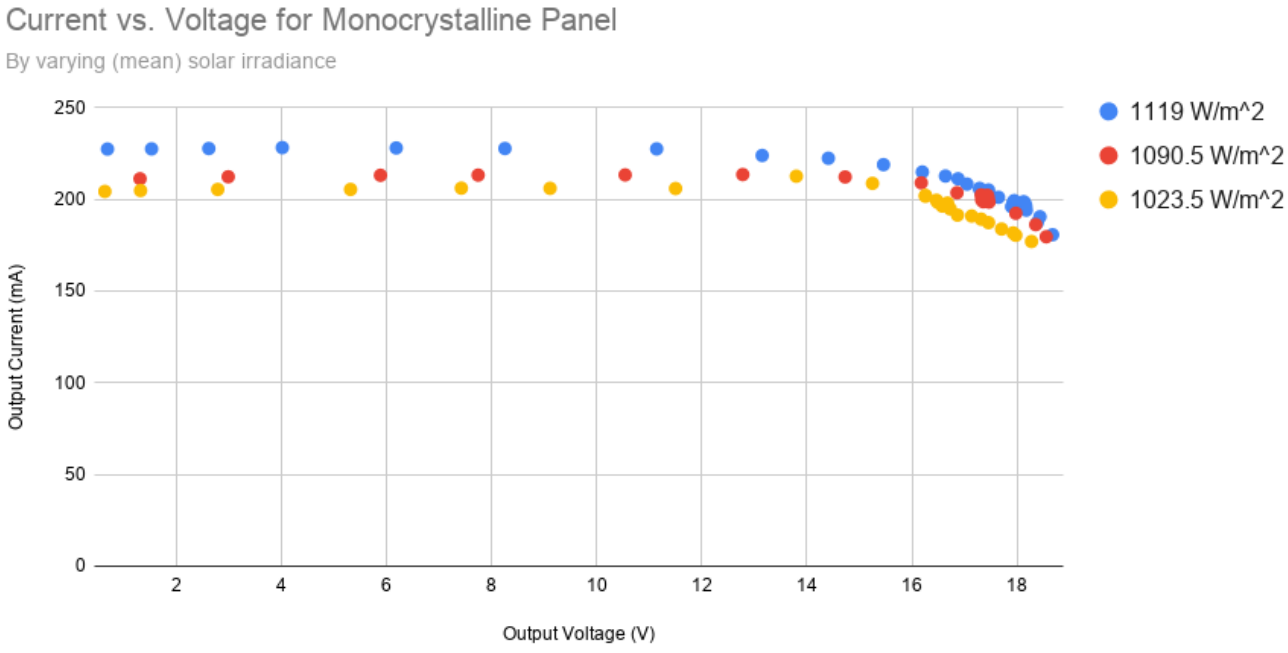

Figure 12: I-V Plots of Multiple Data Sets for Monocrystalline Panel

Each set of experimental data was then simulated using the LabVIEW program. This was done by first inputting the proper basic parameters, such as the band gap, ideality factor, temperature coefficient, etc., then adjusting to the correct conditions of temperature and solar irradiance. The output values from the LabVIEW program of maximum output power, voltage at maximum power, current at maximum power, optimal load resistance, and efficiency were recorded next to their experimental counterparts. Trends were identified and examined in a graphically format.

First, the relationship previously discussed between solar irradiance and output power was also examined using Figure 13. Similar to the analysis with strictly experimental data, this analysis also shows a direct correlation between solar irradiance and output power. But Figure 13 also includes a comparison to the theoretical values given by the LabVIEW simulation. Both the actual and theoretical values of power seem to have a mostly linear relationship to solar irradiance. Furthermore, the theoretical values for power were always greater than their actual counterparts, and differed by approximately the same amount.

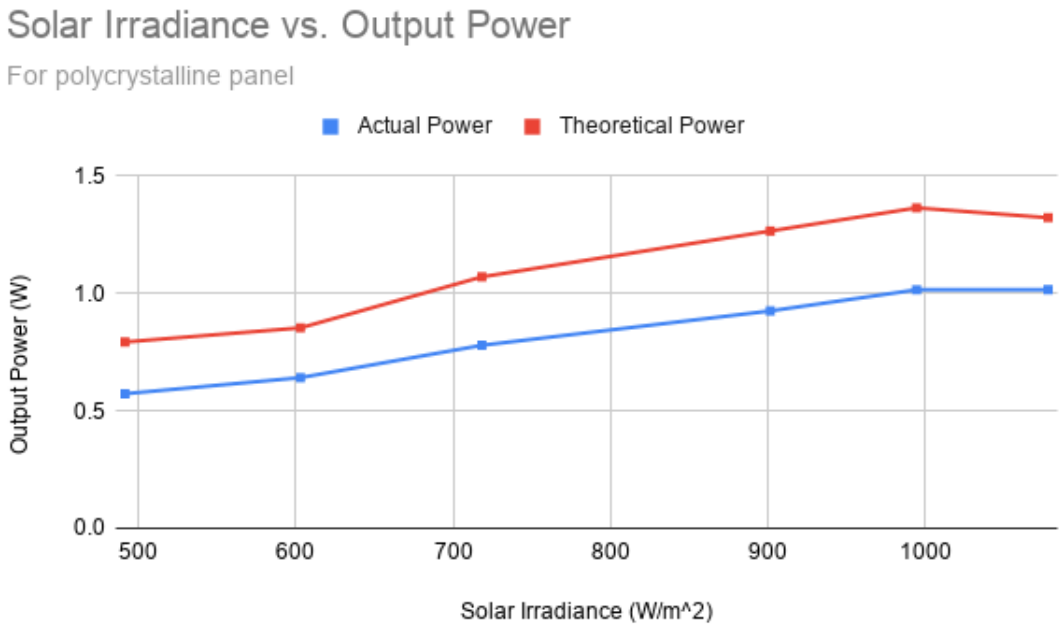

Figure 13: Relationship between Solar Irradiance and Output Power

Next, the relationship between output current and solar irradiance was also plotted. Since output power and current are directly related, it was not surprising that Figure 14 also showed a positive correlation between output current and solar irradiance. This graph in Figure 14 also confirms the expected result that, like output power, the theoretical values for current were always greater than their actual counterparts.

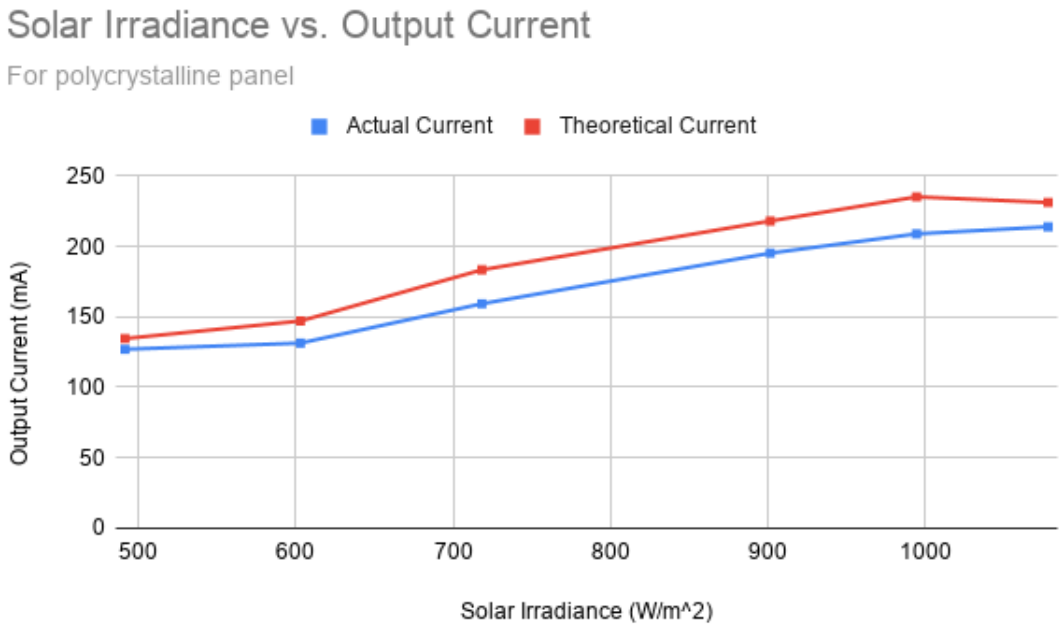

Figure 14: Relationship between Solar Irradiance and Output Current

The next interesting trend revealed from this data analysis was a correlation between solar irradiance and optimal load resistance. The expected results that were hypothesized at the start of this project did not include any relationships regarding optimal load resistance. However, it is clearly shown in Figure 15 that as solar irradiance increased, the optimal load resistance for maximum output power decreased. This relationship holds true for all theoretical data points, and all but one of the actual data points. It is worth noting that while this data point corresponds to a solar irradiance of 491.5 W/m^2 (the lowest recorded solar irradiance), the temperature value for that data set was 303.71 K (the highest recorded temperature). This is one possible explanation for the deviation from the trend. In general,

temperature did not have a consistent correlation to optimal load resistance, as optimal load resistance was more dependent on solar irradiance. However, the significantly higher temperature in combination with an already low solar irradiance may have caused the decrease in maximum voltage output, then causing the optimal load resistance $R = \frac{V}{I}$ to decrease. Nonetheless, the general trend shown in Figure 15 matches the model, given that a higher solar irradiance results in a higher output current, and since $R = \frac{V}{I}$, a higher current results in a lower resistance needed.

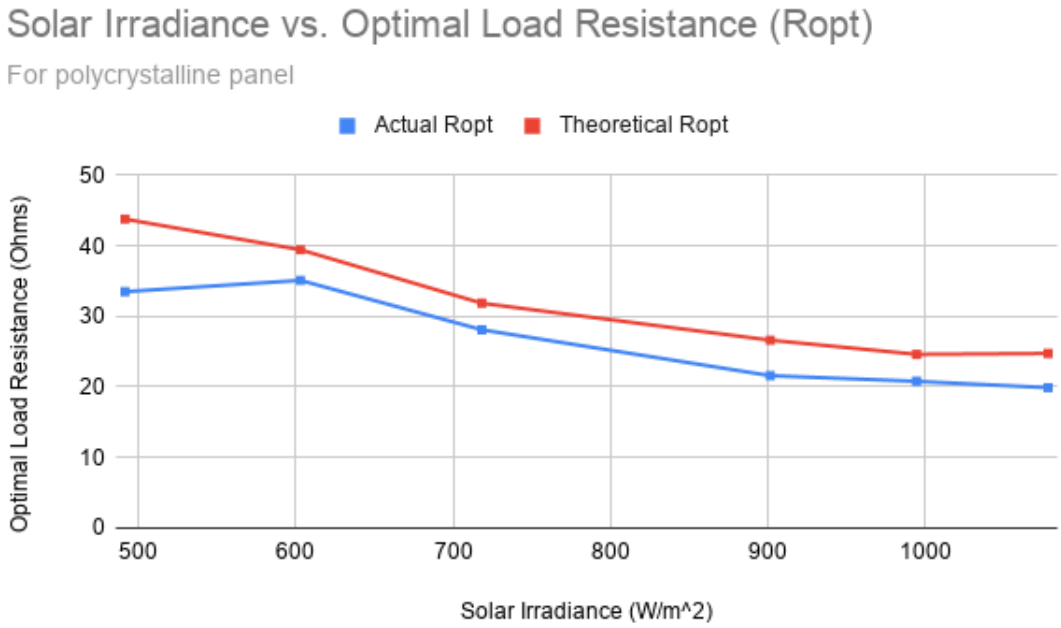

Figure 15: Relationship between Solar Irradiance and Optimal Load Resistance

The last trend that was revealed from this portion of the data analysis was a correlation between temperature and efficiency. As shown in Figure 16, panel efficiency (at least, for the polycrystalline panel) consistently increased with an increase in temperature, independent of solar irradiance. This was first identified with the experimental data, then confirmed with the simulation data. It was surprising that for both theoretical and actual values efficiency increased as temperature increased, since it was initially hypothesized that an increase in temperature would cause efficiency to decrease. Much of the existing literature and research

concludes that temperature has a negative effect on the performance of a PV solar cell, and the general consensus throughout the industry is that the best conditions for PV solar cells are sunnier, colder days [14]. A possible explanation for this finding of a positive correlation between temperature and efficiency was further explored in the third and final portion of data analysis.

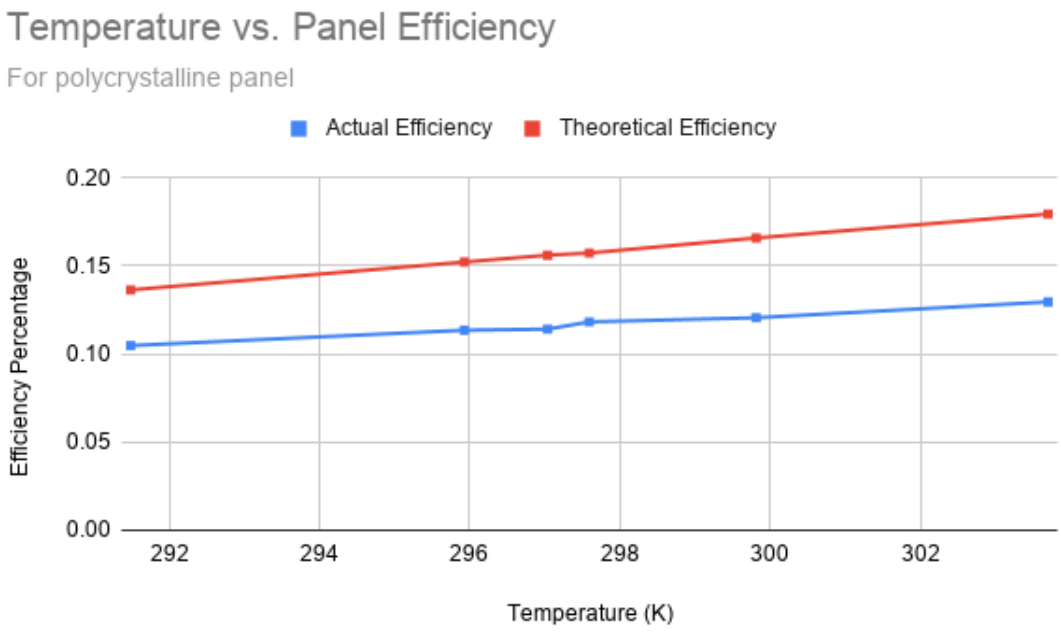

Figure 16: Relationship between Temperature and Efficiency

The final portion of data analysis for this project was strictly simulation based. Using the output values and graphs from the LabVIEW program, the relationships between conditions of solar irradiance or temperature and the I-V and P-V characteristics were evaluated from a strictly theoretical standpoint. The LabVIEW program was especially useful to help explain why the data of this project suggested a positive temperature vs. efficiency relationship when the existing research suggests otherwise. Keeping solar irradiance and all other parameters constant, the temperature was changed to six different values and each P-V and I-V curve was plotted, where the plots go in order of increasing temperature from white to purple.

The first simulation result shown in Figure 17 was generated with the specific parameters for the polycrystalline panel used in this project. Using the manufacturer's data, the short-circuit current and open-circuit voltage at reference temperature of 298.15 K were entered as 0.250 mA and 6.00 V, respectively. Figure 17 shows that when temperature increased, the maximum power output of the cell actually increased. Since solar irradiance was constant, this also shows that efficiency increased. This simulation result confirms the experimental result shown in Figure 16, but both of these findings seem to disagree with the widely accepted statement that higher temperatures negatively affect PV performance.

However, Figure 18 shows one possible explanation for this discrepancy. The same process was repeated, but instead for a "hypothetical" solar panel with a short-circuit of 6.00 A and an open-circuit voltage of 0.600 V at reference temperature of 298.15 K. Again, keeping solar irradiance constant and just changing temperature, Figure 18 shows that an increase in temperature actually correlates to a decrease in maximum power output. This is a different result from the experimental data, suggesting that the short-circuit current and open-circuit voltage characteristics of a PV solar panel can change how it reacts to temperature changes.

Other values of short-circuit current and open-circuit voltage were also tested in the LabVIEW simulation, and similar results were found. This simulation-based data analysis suggests that a solar panel with a larger ratio of short-circuit current to open-circuit voltage, $I_{sc} : V_{oc}$, is more negatively affected by higher temperatures than a solar panel with a small ratio. This explains why the polycrystalline panel used for this project, with a very small $I_{sc} : V_{oc}$ ratio, actually showed an increase in efficiency with a rise in temperature. It also explains why the industry states that solar panels perform better in colder weather, since most of the solar panels for industrial or even home use are much larger in size and are able to generate much more current to produce more power and electricity. Therefore, these panels typically have a much larger $I_{sc} : V_{oc}$ ratio; but unfortunately, that suggests they would be more negatively affected by higher temperatures.

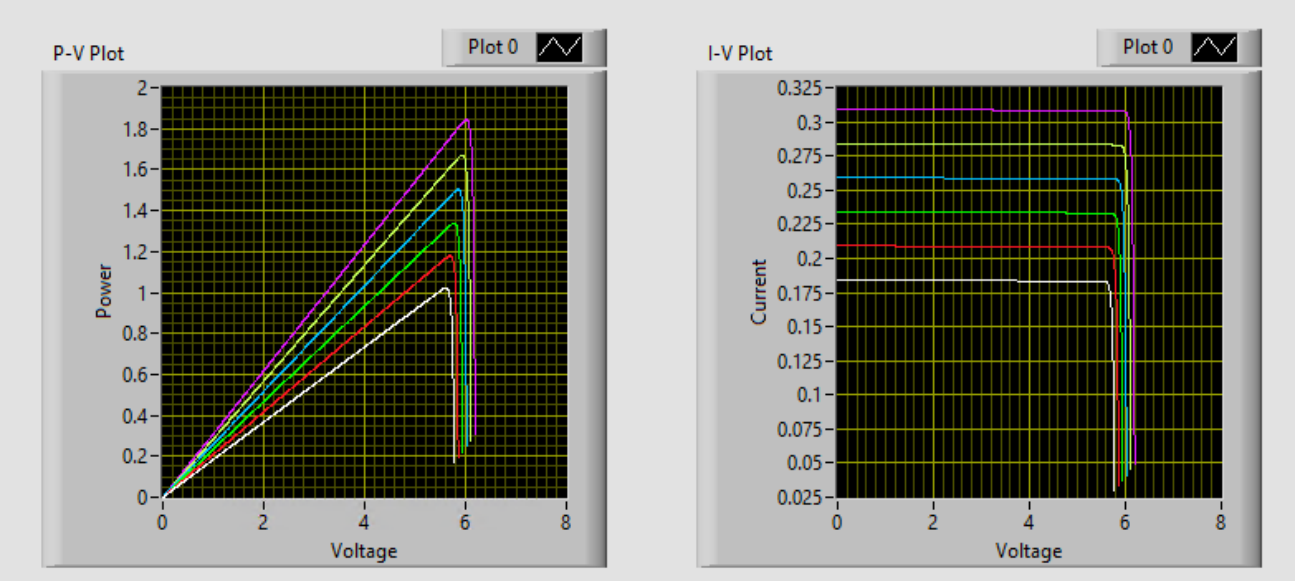

Figure 17: Plots of Varying Temperature in LabVIEW; Small Ratio of $I_{sc} : V_{oc}$

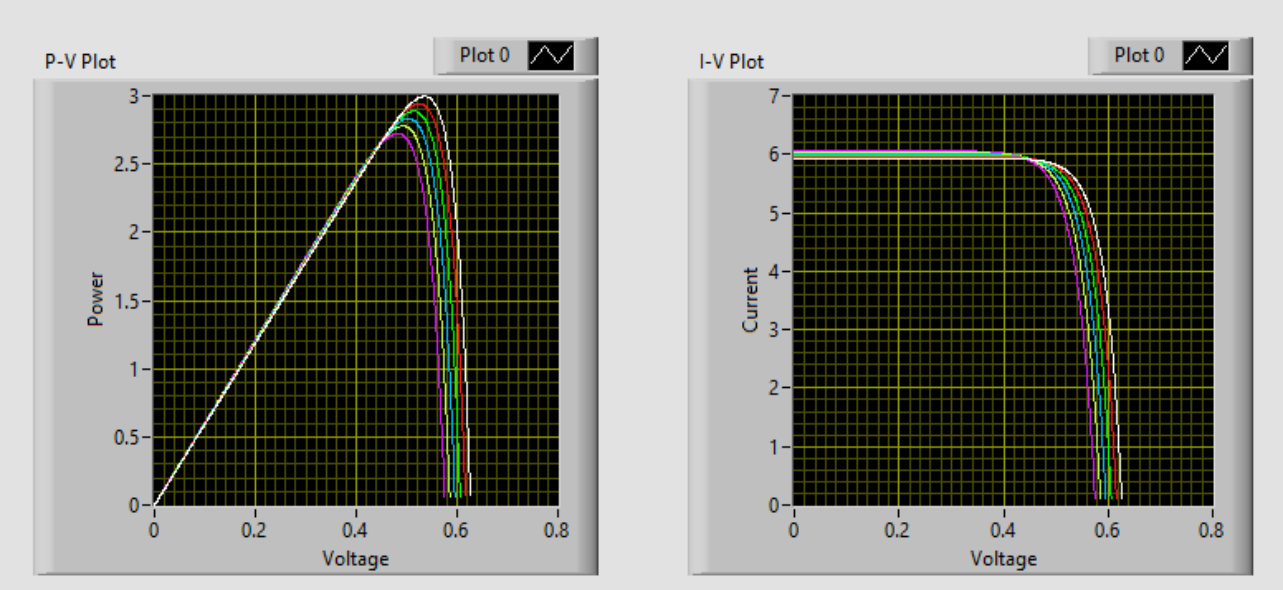

Figure 18: Plots of Varying Temperature in LabVIEW; Large Ratio of $I_{sc} : V_{oc}$

Lastly, the LabVIEW simulation data was also used to confirm the effects of solar irradiance. Keeping all parameters including temperature constant, the solar irradiance was increased to 200, 400, 600, 800, 1000, and 1200 W/m^2 (with plots in increasing order from white to purple). While the ratio of $I_{sc} : V_{oc}$ does slightly change the curvature of the P-V and I-V plots, the important result is the same regardless of the short-circuit current and open-circuit voltage characteristics. As solar irradiance increases, maximum output power increases, as well as the voltage and current at maximum power. This simulation result confirms the experimental results and the original hypothesis.

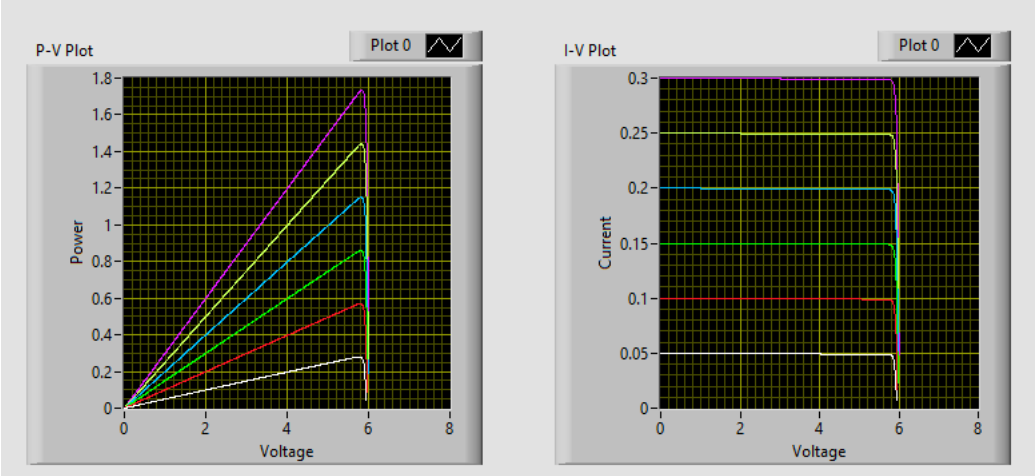

Figure 19: Plots of Varying Solar Irradiance in LabVIEW with Small I_{sc}:V_{oc} Ratio

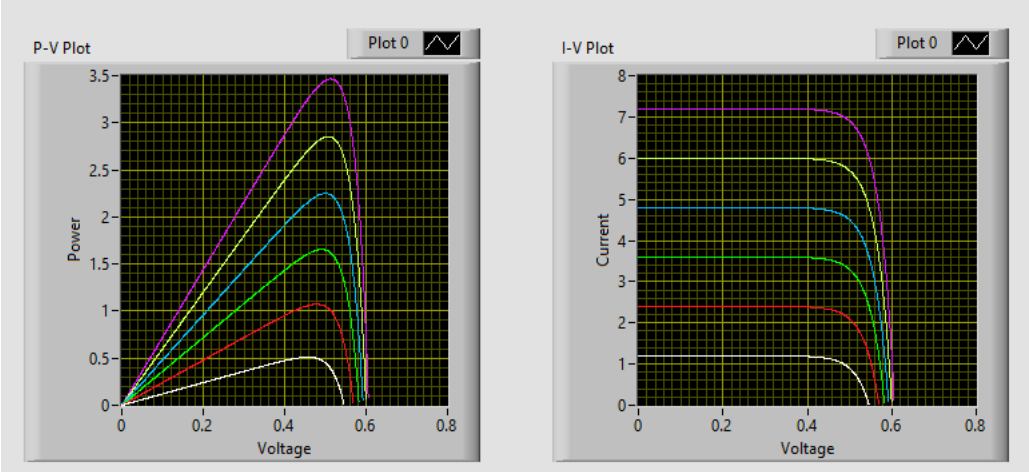

Figure 20: Plots of Varying Solar Irradiance in LabVIEW with Large I_{sc}:V_{oc} Ratio

Discussion

What this data leads to suggest, is that first, solar irradiance is clearly very important for generating more power. The more power that can reach the solar panel, the more power it can possibly output, so it makes sense that the data collected in this project showed a consistently positive correlation between solar irradiance and power output. But unfortunately, not all of the sun's power actually reaches sea level as shown in Figure 21, and of the energy that does, some of it is lost depending on the band gap of the semiconducting material. Silicon has a band gap of about 1.12 electron volts (eV), which is about 1100 nanometers (nm) in wavelength, so photons coming in with wavelengths higher than that do not have enough energy to cause current flow in the panel. So finding materials with different band gaps to allow for use of that higher wavelength light, or finding ways to combine the use of materials with different band gaps may be advantageous. Another area of improvement would be to find protective materials that reflect less light, or find ways to minimize the area of metal contacts on the front of the panel, so that the most sunlight as possible can reach the actual semiconducting material. The metal contacts on the front of the panel are necessary to carry the current generating from the semiconducting material to whatever the panels are connected to, such as a battery, motor, etc. So since the metal contacts cannot be removed completely, there has been research on ways of creating the most efficient metallization designs and patterns that minimize surface area, such as hexagonal or leaf-shaped [15].

The data also leads to suggest that for more practical, larger-scale panels with higher output current, temperature can have negative effects on performance. Like sunlight, heat can also give energy to electrons. So, higher temperatures can raise the energy of the resting electrons causing the potential difference between the resting and excited state to be smaller, so less power is actually generated [14]. A possible extension or future question of this project could then be to investigate if this is related to recombination losses. Recombination occurs when an electron is freed by the photon energy, but the electron recombines with a positive charge known as a "hole" before it makes it into the flow of current. Therefore, recombination

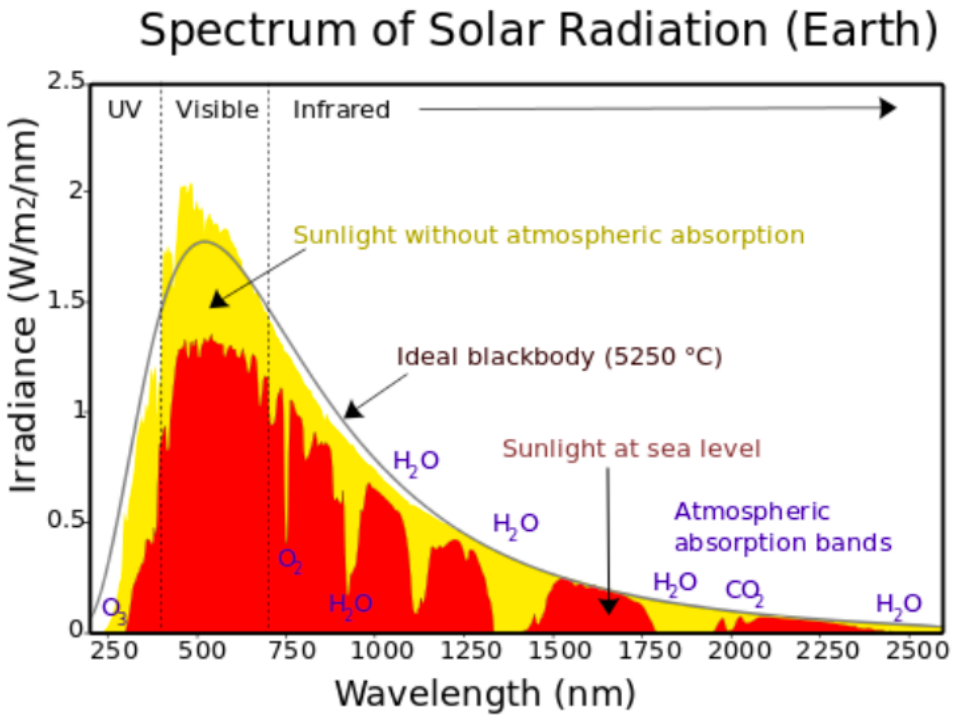

Figure 21: Spectrum of Solar Radiation [16]

results in power losses and negatively affects the performance of a solar cell [1].

To conclude, the results of the project suggest solar irradiance and temperature are two extremely important factors that affect the performance of photovoltaic solar cells. Future research should continue to focus on finding ways for solar panels to optimize the solar irradiance and temperature conditions they operate in. Two practical suggestions then are dynamic power tracking, a technology where the solar panel can move and rotate based on how the sun moves, and active cooling, where some of the electricity generated is actually used to cool the panels to prevent power losses from overheating [17]. Research to make these technologies effective could help improve practical efficiency of solar panels, leading to significant advancements in global energy reliance on renewable, clean photovoltaic solar power.

Appendix

Experimental Circuit Setup

Shown below are the schematics and practical setups for each circuit used in the experimental portion of this project. In each schematic diagram, the solid lines represent what is included to model the PV solar cell (from the equivalent circuit) while the dashed lines represent components to be attached to the PV solar cell.

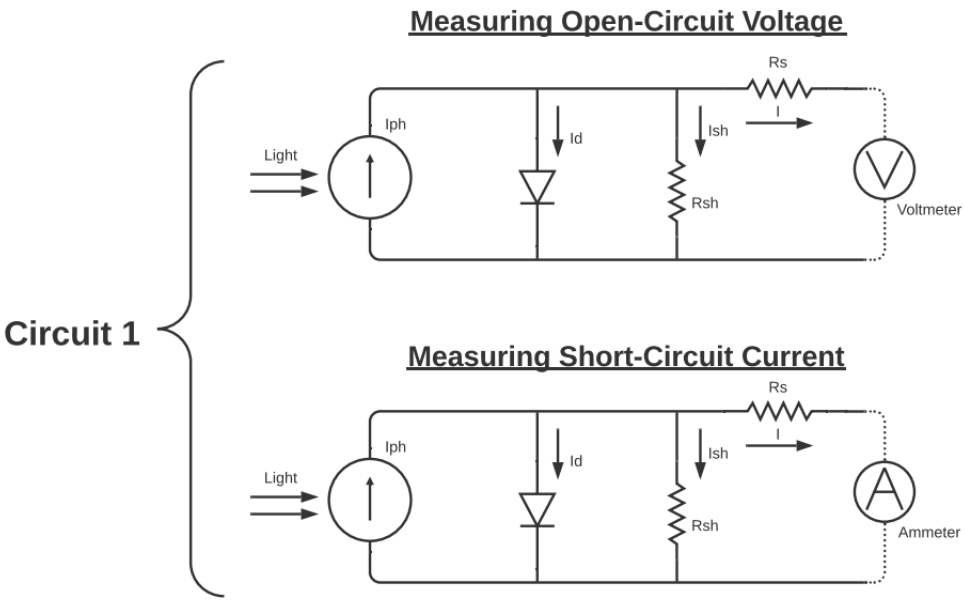

Figure 22: Schematic for **Circuit 1**, used to measure open-circuit voltage and short-circuit current

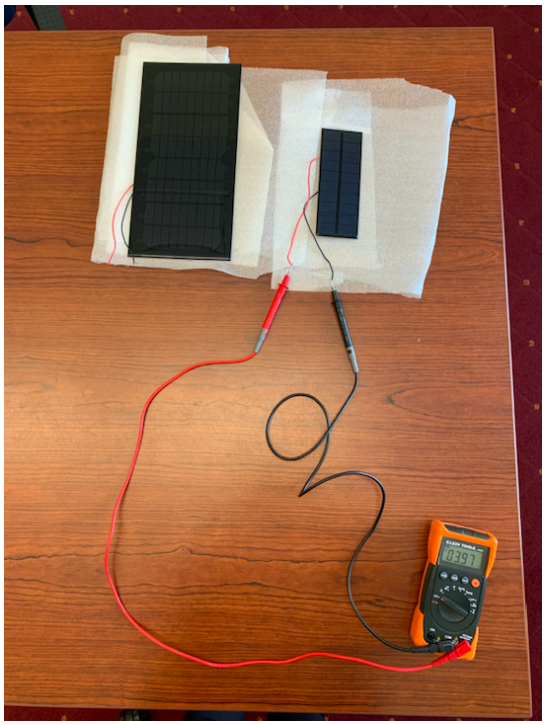

Figure 23: Picture of Practical Setup for **Circuit 1**, used to measure open-circuit voltage and short-circuit current

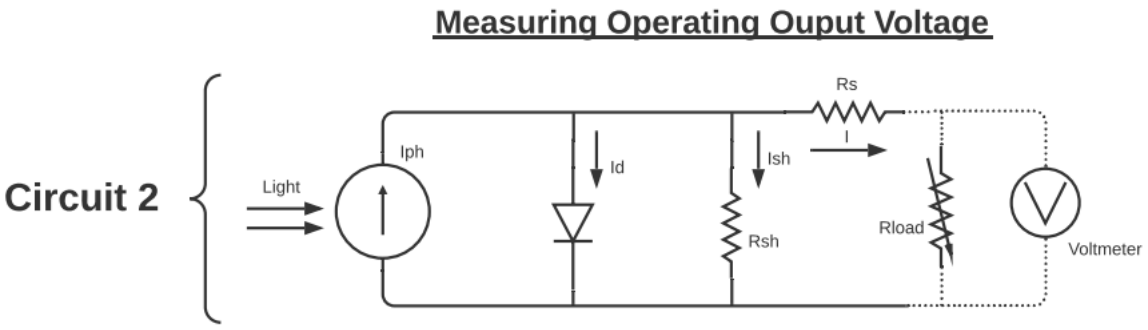

Figure 24: Schematic for **Circuit 2**, used to measure output voltage across the variable load resistance given by the potentiometer

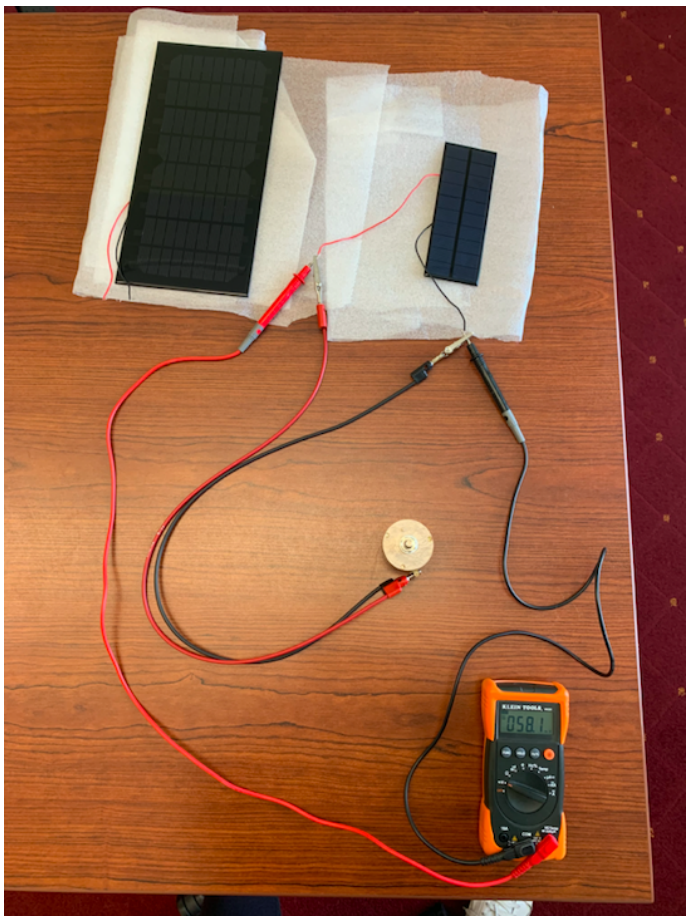

Figure 25: Picture of Practical Setup for **Circuit 2**, used to measure output voltage across the variable load resistance given by the potentiometer

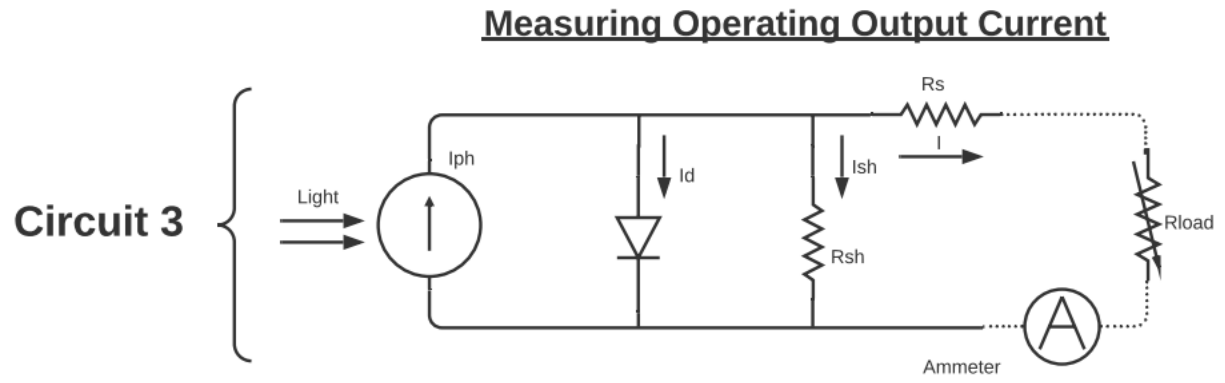

Figure 26: Schematic for **Circuit 3**, used to measure output current through the variable load resistance given by the potentiometer

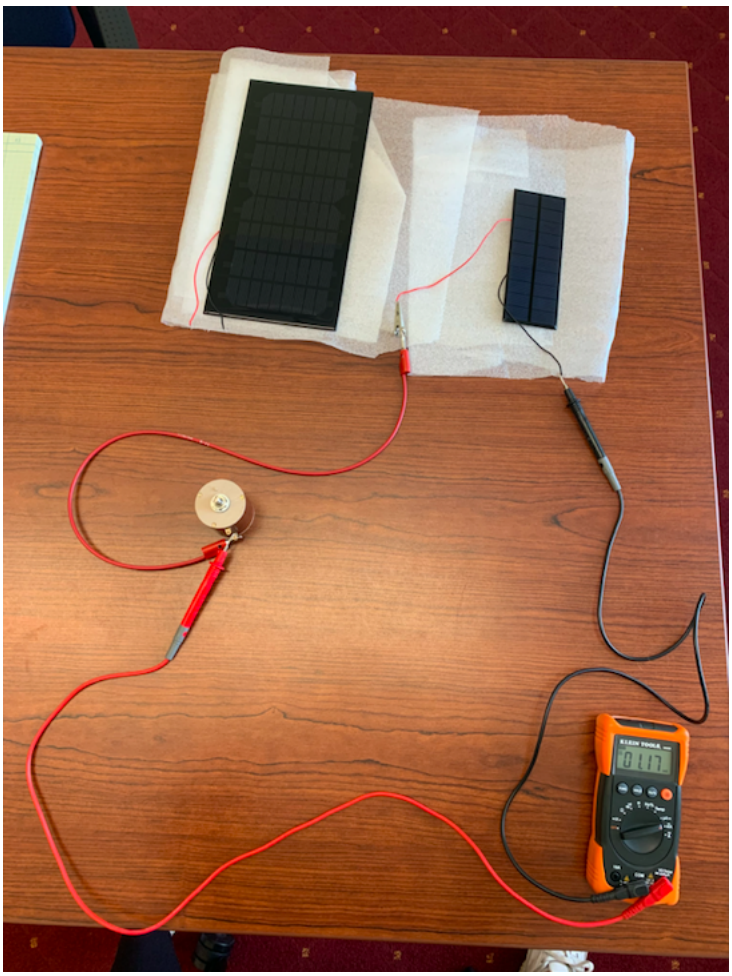

Figure 27: Picture of Practical Setup for **Circuit 3**, used to measure output current through the variable load resistance given by the potentiometer

LabVIEW Program

Shown below in Figure 28 is the flow-chart for the LabVIEW program used for the simulation portion of this project.

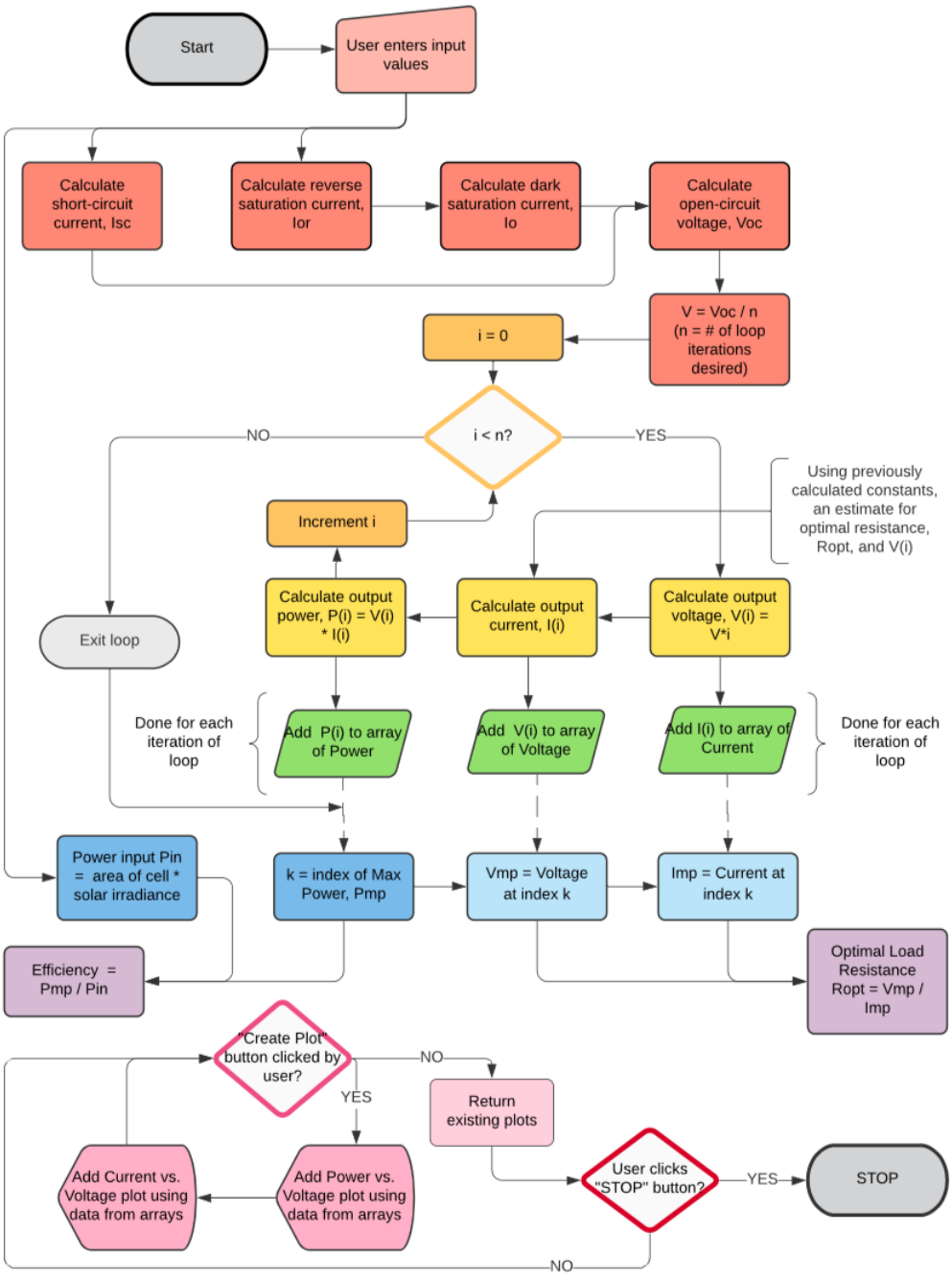

Figure 28: Flow-chart of the LabVIEW program

Shown below in Figure 29 is an example of screenshot of an output of the front panel of the simulation. In this particular image, the data is showing the effects of varying solar irradiance.

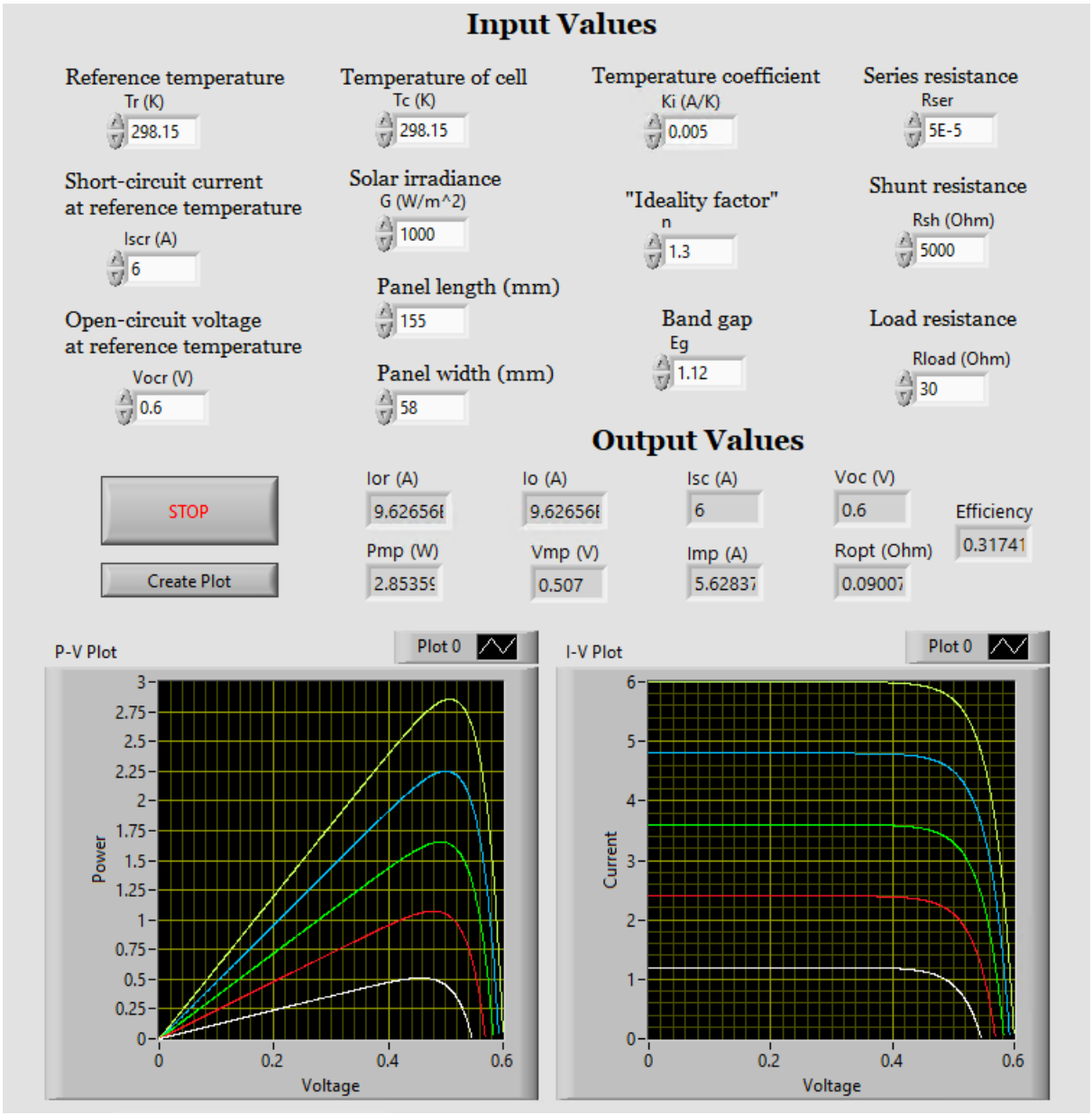

Figure 29: Screenshot of the Front Panel of the LabVIEW Program

References

[1] J. Bisquert, *The physics of solar cells perovskites, organics, and photovoltaic fundamentals* (CRC Press, 2017), Boca Raton.

[2] W. Shockley and H. J. Queisser, "Detailed balance limit of efficiency of p-n junction solar cells", Journal of Applied Physics **32**, 510–519 (1961).

[3] S. Rühle, "Tabulated values of the shockley–queisser limit for single junction solar cellsx", Solar Energy **130**, 139–147 (2016).

[4] A. Polman, M. Knight, E. Garnett, B. Ehrler, and W. Sinke, "Photovoltaic materials: present efficiencies and future challenges", Science **352**, 307–317 (2016).

[5] R. Foster, M. Ghassemi, and A. Cota, *Solar energy: renewable energy and the environment* (CRC Press, 2010), Boca Raton.

[6] *Pn junction theory*, Electronics Tutorials, https://www.electronics-tutorials.ws/diode/diode_2.html.

[7] J. A. Jaleel, A. Nazar, and A. Omega, "Simulation on maximum power point tracking of the photovoltaic module using labview", International Journal of Advanced Research in Electrical, Electronics and Instrumentation Engineering **1**, 190–199 (2012).

[8] E. Meyer, "Extraction of saturation current and ideality factor from measuring *voc* and *isc* of photovoltaic modules", International Journal of Photoenergy **2017**, 1–9 (2017).

[9] M. Kamran, M. Bilal, and Z. Jahanzaib, "Labview based simulator for solar cell characteristics and mppt under varying atmospheric conditions", Mehran University Research Journal of Engineering and Technology **27**, 529–538 (2018).

[10] *Iv curve*, PVEducation, https://www.pveducation.org/pvcdrom/solar-cell-operation/iv-curve.

[11] *Characteristic resistance*, PVEducation, https://www.pveducation.org/pvcdrom/solar-cell-operation/characteristic-resistance.

[12]D. Cotfas, P. Cotfas, and O. Machidon, "Study of temperature coefficients for parameters of photovoltaic cells", International Journal of Photoenergy **2018**, 1–12 (2018).

[13]S. Said, A. Massoud, M. Benammar, and S. Ahmed, "A matlab/simulink-based photovoltaic array model employing simpowersystems toolbox", Journal of Energy and Power Engineering **6**, 1965–1975 (2012).

[14]D. Tobnaghi, R. Madatov, and D. Naderi, "The effect of temperature on electrical parameters of solar cells", International Journal of Advanced Research in Electrical, Electronics and Instrumentation Engineering **2**, 6404–6407 (2013).

[15]D. Gupta, M. Langelaar, M. Barink, and F. van Keulen, "Optimizing front metallization patterns: efficiency with aesthetics in free-form solar cells", Renewable Energy **86**, 1332–1339 (2016).

[16]*The solar spectrum*, Penn State College of Earth and Mineral Sciences, https://www.e-education.psu.edu/meteo300/node/683.

[17]H. Teo, P. Lee, and M. Hawlader, "An active cooling system for photovoltaic modules", Applied Energy **90**, 309–315 (2012).